

Anelastic anomalies and negative Poisson's ratio in tetragonal BaTiO₃ ceramics

Liang Dong,¹ Donald S. Stone,¹ and Roderic S. Lakes^{2,a)}

¹Materials Science Program, University of Wisconsin, Madison, Wisconsin 53706-1687, USA

²Department of Engineering Physics, Engineering Mechanics Program, Materials Science Program, University of Wisconsin, Madison, Wisconsin 53706-1687, USA

(Received 13 February 2010; accepted 18 March 2010; published online 6 April 2010)

Anelastic anomalies (sharp variations in modulus and damping with temperature) were observed in tetragonal BaTiO₃ via broadband viscoelastic spectroscopy after aging at 50 °C for 15 h. The effect was most pronounced under electrical short circuit condition, at low frequency and under small excitation strain (10⁻⁶). Softening in bulk modulus and negative Poisson's ratio were observed near 60 °C. Effects are attributed to an oxygen vacancy mechanism. A relaxational model cannot account for sharp response at smaller strains. Heterogeneity of negative stiffness is considered as a cause. © 2010 American Institute of Physics. [doi:10.1063/1.3384996]

Negative stiffness entails a reaction force in the same direction as imposed deformation. Landau theory predicts a negative bulk modulus during ferroelastic transformation. Inclusions of negative stiffness in a matrix give rise to anomalies (sharp peaks of large magnitude) in modulus and damping.¹ The concept was used to design a particulate composite² of polycrystalline BaTiO₃ in Sn which exhibited extreme anelastic properties (Young's modulus larger than that of diamond) within a narrow range of temperature. Surprisingly, such an extreme response was also observed near 60 °C, which is well outside the normal transformation windows of BaTiO₃ ceramics (125 °C: tetragonal-to-cubic transformation; 5 °C: orthorhombic-to-tetragonal transformation). Such a phenomenon cannot be due to the hindrance of transformation from the constraint of matrix since pure tin will yield at 50 MPa which can merely shift³ the transformation by 2 °C. The present study explores the anelastic anomaly in tetragonal BaTiO₃ ceramic as it depends on strain level, electrical boundary conditions, and frequency. Negative Poisson's ratio of substantial magnitude and softening of the bulk modulus occur at small strain. To our knowledge such effects have not heretofore been experimentally observed in a hard isotropic solid.

Broadband viscoelastic spectroscopy⁴ was used to study the anelastic loss and moduli of three BaTiO₃ specimens (Alfa Aesar, 99.9%, 3~12 mm pieces as received) over a range of temperature with different thermal histories. Deformation of the specimens was induced by electromagnetic torque and measured by a laser method. Data were captured by a lock-in amplifier. Specimens I and II, obtained from one piece, were originally adjacent to each other, and measured as 0.8 × 1 mm² by 9.56 mm (I) and 0.78 × 1 mm² by 8.68 mm (II) after cutting and polishing. Specimen III (0.82 × 1 mm² by 9 mm) was cut from the other piece. Optical microscopy observation reveals a grain size about 25 μm, and domains as small as 1 μm. Gold was sputtered onto all the surfaces of specimen I and III. Specimen II was not coated. Aging was done in air (i) at 50 °C for 15 h and (ii) at 135 °C for 3 h. Each specimen was then cooled freely down to room temperature, at which the temperature was held for

15 min prior to testing. During testing, a thermal rate between 0.008 and 0.01 °C/s was used.

Figure 1(a) shows anomalies in Young's modulus E (absolute value of the complex modulus) and damping $\tan \delta$ in

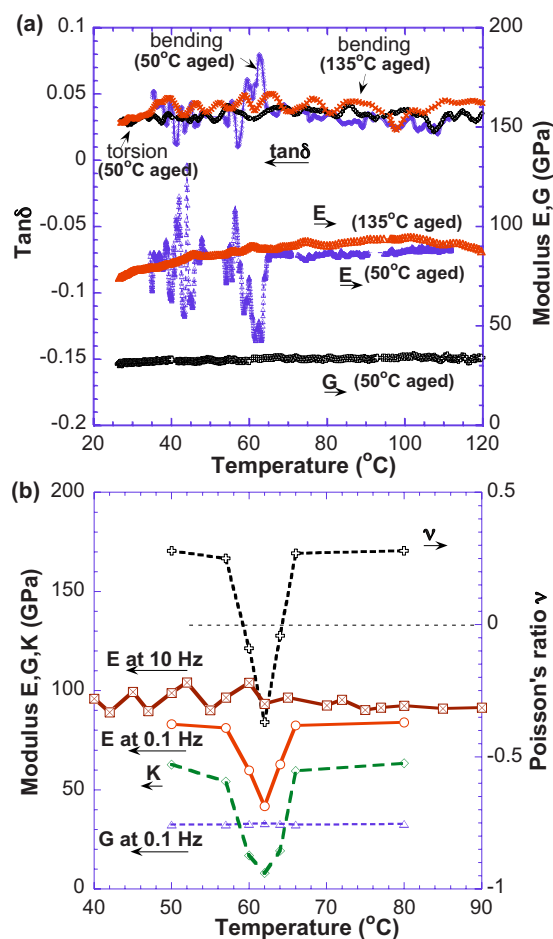


FIG. 1. (Color online) (a) Anelastic anomalies at 0.1 Hz in damping $\tan \delta$ and Young's modulus E outside the normal transformation windows in specimen I (aged at 50 °C). Responses in bending (E) after aging at 135 °C and in torsion (G) after aging at 50 °C are provided as comparison. (b) Bulk modulus K and Poisson's ratio ν calculated from a restricted set of points from (a). E at 10 Hz (after aging at 50 °C) and 0.1 Hz are compared for specimen I. Strain applied is 4×10^{-6} .

^{a)}Electronic mail: lakes@engr.wisc.edu.

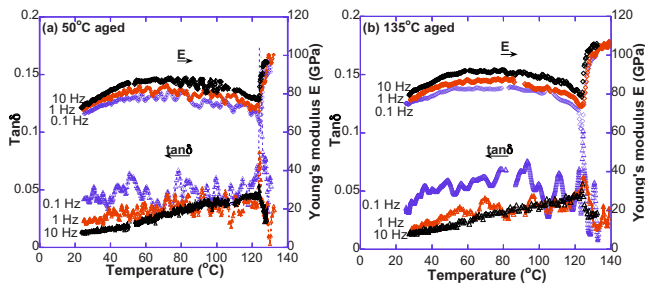


FIG. 2. (Color online) Anelastic response (damping $\tan \delta$ and Young's modulus E): anomalies in specimen III at several frequencies (0.1, 1, and 10 Hz) at a strain of 4×10^{-6} after aging at (a) 50 and (b) 135 °C.

bending observed at an excitation strain of 4×10^{-6} in specimen I after aging at 50 °C. Figure 1(a) also includes the shear modulus G in torsion under the same condition. No anomaly was observed in bending after aging⁵ at 135 °C or in shear. Bulk modulus K and Poisson's ratio ν calculated within a restricted temperature window for selected data points disclose significant softening in bulk modulus and negative Poisson's ratio [Fig. 1(b)]. Anomalies were also observed in uncoated specimen II (between 25 and 40 °C) after aging at 50 °C, but less in magnitude than coated specimen I. Softening of single elasticity tensor elements is well known, but cooperative effects leading to softening of the bulk modulus of stiff materials, is much less so.

Modulus and damping versus temperature at various frequencies of fresh (prior to thermal cycling through the Curie point) specimen III at an excitation strain of 4×10^{-6} is shown in Fig. 2 [(a) aged at 50 °C; (b) aged at 135 °C]. Anelastic anomalies were observed from 55 to 100 °C after aging at 50 °C. Anomalous response becomes more pronounced at lower frequency but there is no shift in temperature with frequency. Specimens I and III both show anomalies but the magnitude and position differ. Such difference can result from heterogeneity in domain textures, defect concentrations or surface strain.⁶

The anelastic anomalies at low strain do not shift in temperature with frequency. The anomalies tend to decrease with increasing applied strain until the broad peaks are observed in damping at an excitation strain of 2×10^{-5} (Fig. 3). Without the superimposed sharp anomalies observed at smaller strain, these broad peaks are relaxational in nature: the peak shifts with temperature according to an Arrhenius relation. Activation energy is about 0.6 eV in specimen II, and 0.8 eV in specimen I. The relaxation time is about 7×10^{-11} s in specimen II and 8×10^{-12} s in specimen I. The activation

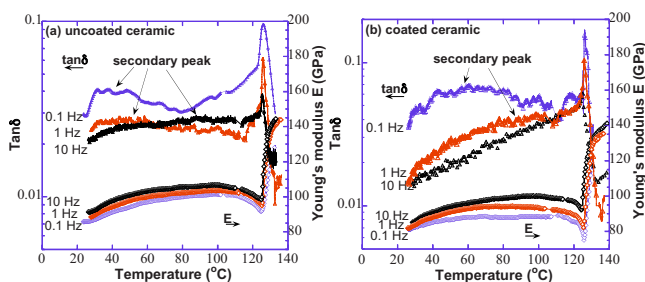


FIG. 3. (Color online) Anelastic response (damping $\tan \delta$ and Young's modulus E) of specimen II (a) and specimen I (b) at a strain of 2×10^{-5} at different frequencies after aging at 50 °C. Results show the relaxation peaks in the damping curves.

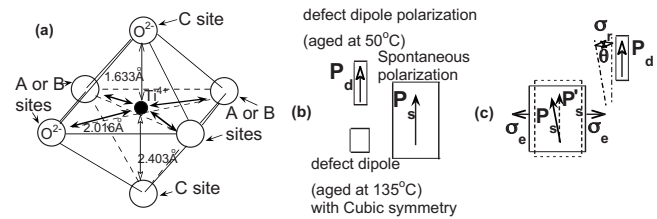


FIG. 4. (a) Oxygen octahedron in tetragonal BaTiO_3 unit cell. O^{2-} has two kinds of nonequivalent sites A or B and C. In cubic phase, the distances between Ti^{4+} and A (B) and C sites are the same. In the tetragonal phase, distances between Ti^{4+} and A (B) and C sites are given (Ref. 7). (b) presents an 180° domain. After aging at 50 °C, \mathbf{P}_d is generated, \mathbf{P}_s and \mathbf{P}_d are aligned in the same direction. After aging at 135 °C, \mathbf{P}_d is not generated shortly after temperature is reduced through the Curie point, and defects possess cubic symmetry. (c) When stress is applied, \mathbf{P}_s will align θ with respect to \mathbf{P}_d and leads to a restoring stress σ_r between \mathbf{P}_s and \mathbf{P}_d .

energies and the relaxation times of the broad peaks are reasonable compared with Ref. 7: $0.5 \sim 0.6$ eV, $2 \times 10^{-11} \sim 2 \times 10^{-9}$ s, measured in an electrical open circuit condition.

Oxygen vacancy (OV) is known to give rise to broad relaxation peaks⁷ in damping near 60 °C in BaTiO_3 . The peaks depend on thermal history and their magnitude depends on OV concentration.⁸ Shift of the peaks to higher temperature in the coated ceramic in comparison with uncoated is attributed to the electrical boundary conditions: the reduced depolarization field enhances the internal polarization which increases the activation energy associated with relaxation process of OVs.

The oxygen octahedron in tetragonal BaTiO_3 unit cell is illustrated in Fig. 4(a). Spontaneous polarization \mathbf{P}_s exists below the Curie point. Impurities, such as Al^{3+} , will preferably locate at Ti^{4+} site, and form defect dipoles⁹ with OVs. According to the mechanism of symmetry-conforming property of point defects (SCP-PD),¹⁰ OV can occupy either of A (B) or C sites of the oxygen octahedron with identical conditional probabilities above the Curie point. Below the Curie point, OV tends to migrate to and accumulate at C sites, which are closer to the center of octahedron, from A (B) sites during aging, and hence forms defect dipole moment \mathbf{P}_d . \mathbf{P}_d will generate a restoring stress on the spontaneous polarization \mathbf{P}_s , forcing \mathbf{P}_s and \mathbf{P}_d to align along the same direction. Aging at 50 °C for 15 h allows \mathbf{P}_d to align in the same direction as \mathbf{P}_s , giving rise to stored energy. In contrast, freely cooling to room temperature from 135 °C (after aging at 135 °C) takes less than 3 min. Such a time interval is too short for \mathbf{P}_d to be generated after passing through the Curie point. Therefore, interactions between \mathbf{P}_s and \mathbf{P}_d will be introduced after aging at 50 °C but not after aging at 135 °C.

Properties with sharp dependence on temperature cannot be explained by a relaxation process. Sharp frequency dependence observed in heterogeneous systems is explained via composite analysis by inclusions of negative stiffness.¹¹ A possible mechanism for negative stiffness to occur based upon SCP-PD in tetragonal BaTiO_3 is as follows. Figure 4(b) presents an 180° domain. Angle θ between polarizations \mathbf{P}_s and \mathbf{P}_d will occur instantaneously when axial stress applies which breaks crystal symmetry [Fig. 4(c)]. Due to the time delay between \mathbf{P}_s and \mathbf{P}_d , a restoring stress σ_r will be introduced. If σ_e (local stress due to applied stress) attains $\sigma_e = \sigma_r$ at a critical angle θ_c , then as θ increases due to inertia of domain walls (DWs), σ_r will be larger than σ_e , and the polarization vector will tend to snap-back due to the nonlinear

interaction between dipoles. At this point, the domain will exhibit a negative stiffness behavior due to release of stored energy as it shrinks under tensional stress. 90° domains cannot switch in polycrystalline ceramics,¹² so cannot cause negative stiffness. The mechanical and electrical conditions within such localized regions are very complex in polycrystalline materials, and are highly coupled with domain textures, dislocation substructures, and thermal conditions. Suitable combination of these factors, which determines stresses σ_e and σ_r and hence entails negative stiffness, may only be satisfied within certain temperature regions.

As for energy of interaction, given Young's modulus of 90 GPa, a strain of 2×10^{-5} corresponds to σ_e of 1.8 MPa. Therefore, for a unit cell volume, the elastic energy induced by excitation strain is on the order of 10^{-21} J. Interaction energy (W) between a defect dipole moment (μ_{defect}) and a spontaneous polarization dipole moment ($\mu_{\text{spontaneous}}$) can be calculated by the equation¹³

$$W = \frac{\mu_{\text{defect}} \mu_{\text{spontaneous}}}{4\pi\epsilon_0 r^3},$$

r is the distance between dipoles (on the order of lattice parameter), and ϵ_0 is vacuum permittivity. Assuming μ_{defect} and $\mu_{\text{spontaneous}}$ to be¹⁴ 6.5×10^{-30} C m, W is on the order of 10^{-21} J, which is consistent with the elastic energy per unit cell volume induced by the applied strain. In real case, such negative stiffness microregion could be entailed within two or three unit cell volumes.¹⁵ An even higher excitation strain will lead to more elastic energy, which is higher than the interaction energy between defect dipole polarization and spontaneous polarization, negative stiffness thus disappears. It is equally to say that when $\sigma_e > \sigma_r$ (σ_r is coercive stress) during the elastic reorientation history of 180° domains, negative stiffness will not occur.

Heterogeneity of negative stiffness gives rise to anomalies in modulus and damping.¹ Undulations in material properties have been predicted in heterogeneous materials with a distribution of negative stiffness values for the inclusions.¹⁶ Such inclusions can be incorporated by design, and have been predicted to appear naturally on a fine scale.¹⁷ For BaTiO₃ ceramic, impurities and vacancies cause heterogeneity via electromagnetic interaction with DWs. No anomaly is observed in shear since there is no volume change, so no deviation between \mathbf{P}_s and \mathbf{P}_d .¹⁸ The magnitude of the anelastic anomaly is less in the uncoated specimen II than in the coated specimen I: the depolarization field will significantly reduce the magnitude of polarization, so the restoring stress between \mathbf{P}_s and \mathbf{P}_d will be less than in a short circuit condition.

Such anelastic anomaly is encouraging in the context of designed materials: one may use different ferroelastic materials, dope proper acceptor ions and utilize heat treatments to attain external damping or negative stiffness at desired temperatures for various applications. The anomalies are pertinent to conventional applications of ferroelectrics in that they may affect the performance of devices.

In conclusion, softening in bulk modulus, negative Poisson's ratio, and anomalies in damping and Young's modulus are observed in tetragonal BaTiO₃. The effects are attributed to an OV mechanism. The sharp dependence of properties on temperature at small strain cannot be explained via a relaxational mechanism. A mechanism based on release of stored energy from negative stiffness heterogeneity is proposed.

Support by NSF-funded MRSEC seed grant (DMR-0520527) is gratefully acknowledged.

¹R. S. Lakes, *Phys. Rev. Lett.* **86**, 2897 (2001).

²T. Jaglinski, D. Kochmann, D. S. Stone, and R. S. Lakes, *Science* **315**, 620 (2007).

³W. J. Merz, *Phys. Rev.* **78**, 52 (1950).

⁴T. Lee, R. S. Lakes, and A. Lal, *Rev. Sci. Instrum.* **71**, 2855 (2000).

⁵Several hours' aging above the Curie point is not necessarily to achieve full rejuvenation (full rejuvenation means defect polarization completely disappears which requires fairly long aging above the Curie point), yet is sufficient to eliminate the anelastic anomalies, and this could be attributed to a low enough volume fraction of the regions containing defect dipoles. Accumulative effect of partial rejuvenation is responsible for the weakening of anelastic anomalies observed in the 50°C aged specimen after extensive thermal cycling through the Curie point.

⁶R. Loetzsch, A. Lubcke, I. Uschmann, E. Forster, V. Große, M. Thuerk, T. Koettig, F. Schmidl, and P. Seidel, *Appl. Phys. Lett.* **96**, 071901 (2010).

⁷L. Chen, X. M. Xiong, H. Meng, P. Lv, and J. X. Zhang, *Appl. Phys. Lett.* **89**, 071916 (2006).

⁸B. L. Cheng, M. Gabbay, M. Maglione, Y. Jorand, and G. Fantozzi, *J. Phys. IV* **6**, 647 (1996).

⁹Manufacturer analysis (Lot number: I27Q015) shows concentrations Al < 0.001%; Mg, Ca, Si < 0.001%; Sr < 0.03%. Various types of impurities can form defect dipoles with OV, and provide restoring stress on \mathbf{P}_s , according to Ref. 10. In addition, Ti⁴⁺ can reduce to lower valence Ti³⁺, form defect dipole with OV. BaO (theory): 65.74 %; BaO (found) 65.41 %; TiO₂ (theory) 34.26 %; TiO₂ (found) 34.25 %.

¹⁰X. B. Ren, *Nature Mater.* **3**, 91 (2004).

¹¹L. Dong, D. S. Stone, and R. S. Lakes, *J. Appl. Phys.* **107**, 023514 (2010).

¹²J. Y. Li, R. C. Rogan, E. Ustundag, and K. Bhattacharya, *Nature Mater.* **4**, 776 (2005).

¹³C. J. F. Bottcher, *Theory of Electric Polarization* (Elsevier, Amsterdam, 1952).

¹⁴W. J. Merz, *Phys. Rev.* **91**, 513 (1953).

¹⁵L. X. He and D. Vanderbilt, *Phys. Rev. B* **68**, 134103 (2003).

¹⁶T. Jaglinski, D. S. Stone, and R. S. Lakes, *J. Mater. Res.* **20**, 2523 (2005).

¹⁷K. Yoshimoto, T.S. Jain, K.V. Workum, P.F. Nealey, and J. J. de Pablo, *Phys. Rev. Lett.* **93**, 175501 (2004).

¹⁸X. Ren and K. Otsuka, *Nature (London)* **389**, 579 (1997).